Stabilization of Reduced Primary Quinone by Proton Uptake in Reaction Centers of *Rhodobacter sphaeroides*†

László Kálmán and Péter Maróti*

Institute of Biophysics, Jôzsef Attila University Szeged, Egyetem utca 2. Szeged, Hungary, H-6722

Received March 10, 1994; Revised Manuscript Received May 23, 1994®

ABSTRACT: Proton binding stoichiometry and kinetics of charge recombination were measured after single flash excitation in reaction centers from the purple photosynthetic bacterium, *Rhodobacter sphaeroides* strain R-26, where the native ubiquinone in the primary quinone acceptor site Q_A was removed and replaced by (benzo-, naphtho-, and anthra-) quinones of various structures and redox midpoint potentials. The observed proton binding stoichiometry was small (0.2–0.4 H^+/Q_A^-) and not specific to quinones in the acidic and neutral pH ranges. Above pH 9, however, significant differences were detected; reaction centers reconstituted by menadione failed to take up protons above pH 9.5. The pH dependence of the free energy change (stabilization) of the semiquinone was determined by integration of the proton uptake stoichiometry as a function of pH. Ubiquinone had the largest (100 meV at pH 5) and menadione the smallest (49 meV at pH 5) stabilization energy compared to those at very high (>11) pH. In the case of the anthraquinone-reconstituted reaction center, acceptable agreement was obtained above pH 9 for the stabilization energies derived from energetic parameters of the thermally activated electron transfer (back reaction) and from proton binding stoichiometries. The stabilization at high pH could be attributed to a single protonatable amino acid, which might be either in the Q_B (secondary quinone) pocket (Glu L212) or in the vicinity of the Q_A binding domain (Tyr H40). It was shown that this residue had a negligible energy of interaction with bacteriopheophytin and that its coupling to the semiquinone was sensitive to the structure and physicochemical properties of Q_A. The possibilities are discussed in terms of long-range electrostatic interactions and solvent accessibility based on the three-dimensional structure of the reaction center.

The primary steps of the conversion of light into chemical free energy in photosynthesis occur in a specially organized membrane protein called the reaction center (RC).[1] The amino acids of the three subunits (L, M, and H) and the nine cofactors of the RC of the purple bacterium *Rhodobacter* (*Rb.*) *sphaeroides* have been localized with atomic resolution (Allen et al., 1986, 1988; Chang et al., 1986; Arnoux et al., 1989). The absorbed light in the bacteriochlorophyll dimer initiates the transfer of an electron to the primary stable acceptor quinone via bacteriopheophytin and further transfer to the secondary acceptor quinone if available. The forward electron transfer competes with charge recombination, and the mechanisms of stabilization of the separated charges are key problems in understanding the primary processes. The electron transfer is accompanied by the uptake of protons that results in a proton gradient, the driving force for ATP formation. As the two electrons and two protons are delivered to Q_B to form completely reduced (dihydro)quinone, the protonation of Q_B has been discussed at great length in the literature [for recent reviews, see Okamura and Feher (1992) and Maróti (1993)]. In contrast, the proton uptake associated with Q_A reduction has not been the subject of as much attention. The problem, however, is of great importance as it is related to the very first step of the light-activated proton-pump mechanism and/or to the production of the first stable intermediate ($P^+Q_A^-$) in photosynthesis.

Early spectroscopic (Clayton & Straley, 1972) and recent direct proton binding measurements on strains R-26 (Maróti & Wraight, 1988; McPherson et al., 1988) indicated that (similar to Q_B^-) Q_A^- is not protonated directly. The observed proton uptake could be attributed to the p*K* shifts of (at least four) protonatable amino acids in interaction with Q_A^-. The primary quinone performs one-electron chemistry and is fixed in a highly apolar and aprotic environment that contains several aromatic amino acids. There is no protonatable residue in the 12-Å vicinity of Q_A. The secondary quinone, on the other hand, undertakes two-electron chemistry and is surrounded by a cluster of acidic residues. In their charged states, these amino acids have a free energy of interaction with Q_B^- of greater than 200 meV (Gunner & Honig, 1992). Electrostatic control of the quinone redox state, however, may operate over long distances [see, for example, photorevertants: Hanson et al. (1993) and Maróti et al. (1994)], and distant protonatable groups can participate in the stabilization of the Q_A semiquinone form.

Proton binding induced by the anionic semiquinone Q_A^- is the response of the protein to the appearance of a negative charge in order to compensate for or solvate it. The dielectric does not tolerate a negative charge on Q_A without solvation. Several earlier (Kleinfeld et al., 1984a) and recent results (Brzezinski et al., 1992; Tiede & Hanson 1992; Kálmán et al., 1993) indicate that there are structural alterations that stabilize the $P^+Q_A^-$ charge-separated state, and these conformational changes are related, at least in part, to fast protonation to accommodate the quinone in its reduced form.

Removal of the native quinone Q_A from the RC of *Rb. sphaeroides* and replacement of it with other quinones with different structures and/or redox potentials, have been a useful

† Work was supported by the Hungarian Science Foundation (OTKA 1978–1991). P.M. thanks the European Community for a short-term fellowship (PECO) in CNRS CGM Photosynthese Bacterienne, Gif/Yvette, France.

* Author to whom correspondence should be addressed.

® Abstract published in *Advance ACS Abstracts,* July 1, 1994.

[1] Abbreviations: P, bacteriochlorophyll dimer; I, bacteriopheophytin; Q_A, primary quinone acceptor; Q_B, secondary quinone acceptor; AQ, anthraquinone; 1-Cl-AQ, 1-chloroanthraquinone; DQ, duroquinone; MD, menadione; 1,4-NQ, 1,4-naphthoquinone; UQ_{10}, ubiquinone-50; RC, reaction center.

0006-2960/94/0433-9237$04.50/0

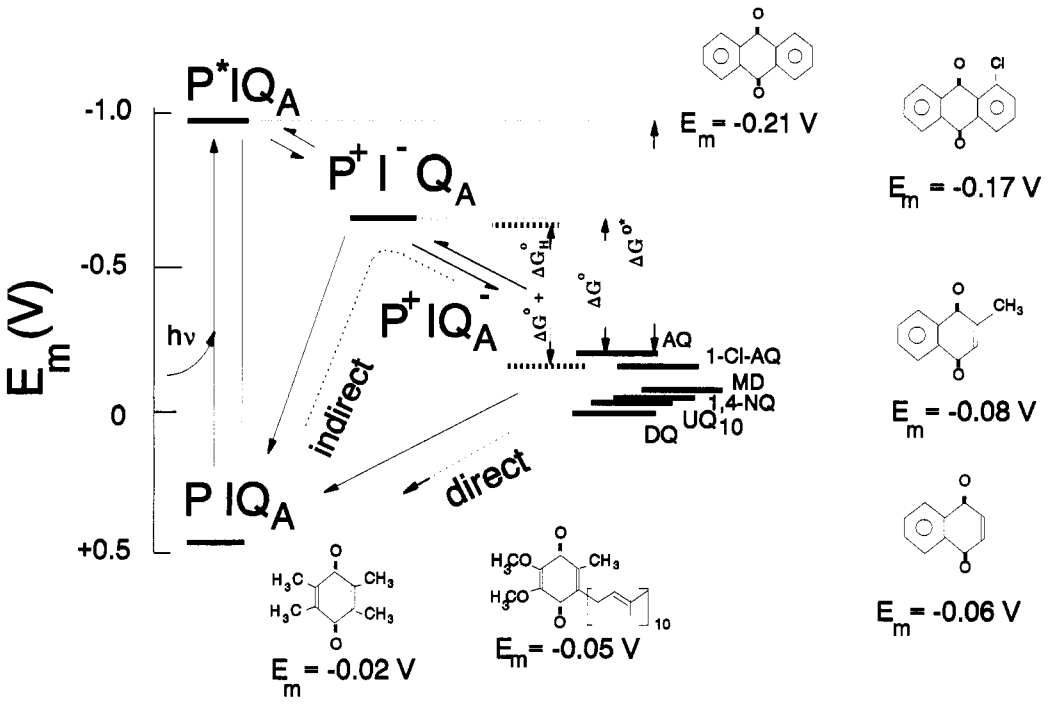

FIGURE 1: Energetics of flash ($h\nu$)-induced charge separation reactions, leading to the formation of $P^+IQ_A^-$, the pathways for charge recombination in the isolated RC protein of *Rb. sphaeroides* together with the in situ redox midpoint potentials (E_m) at pH 8 (Woodbury et al., 1986), and chemical structures of various quinones used for the reconstitution of Q_A activity in this study. The pH-dependent stabilization of states $P^+I^-Q_A$ and $P^+I(AQ)_A^-$ is illustrated by dashed lines. For simplicity, the reactions involving Q_B, as well as routes yielding triplet states of the primary donor, P, are omitted.

approach to study the thermodynamics of the RC and the mechanisms of forward and backward electron transfer reactions (Okamura et al., 1975; Gunner et al., 1986; Woodbury et al., 1986; Feher et al., 1988; Sebban 1988a,b; Liu et al., 1991). These studies, however, have not involved direct proton binding measurements. The question arises concerning whether the proton uptake induced by reduction of the primary acceptor is influenced by the redox and/or steric properties of the quinone. To study this problem, a set of quinones of low and high redox potentials and different ring sizes was used to reconstitute the UQ-depleted RCs into the Q_A^--binding site (Figure 1).

Kinetic and energetic parameters were determined from electron transfer (charge recombination) characteristics and proton binding stoichiometries. We compared the free energy of stabilization determined from both electron transfer and associated proton uptake in anthraquinone-reconstituted RC and found reasonable agreement at pH values above 9. We obtained significantly different proton binding stoichiometries vs pH dependence (i.e., different stabilization energies) with various quinones. The electrostatic influence of Q_A^- and I^- on Tyr H40 and the acidic cluster in the Q_B pocket as the dominating interaction for proton uptake at high pH (>9.5) is discussed, but not solved.

EXPERIMENTAL PROCEDURES

Reaction Center Preparation. Reaction centers from *Rb. sphaeroides* strain R-26 were isolated by detergent fractionation of chromatophore membranes with LDAO (*N,N*-dimethyldodecylamine *N*-oxide, Fluka) followed by ammonium sulfate precipitation and ion-exchange column chromatography on DEAE-Sephacel (Sigma), as previously described (Maróti, 1991a). RCs were eluted from the DEAE-Sephacel column with 200 mM NaCl/0.1% LDAO/10 mM Tris (pH 8.0). The purity of the RC was checked by absorbance measurements and an observed ratio of $A(280)/A(802) < 1.30$ was found.

Q-Depletion Column Material. The Q-depletion column was prepared by incubating the DEAE-Sephacel in TL buffer (10 mM Tris, 0.1% LDAO, and 1 mM EDTA (Serva), pH 8.0) with 1 mg/mL BSA (bovine serum albumin, Reanal), at 27 °C for 1 h. The unbound BSA was removed with 0.5 M NaCl in TL buffer, and the NaCl was eliminated by TL buffer.

Q-Depleted RCs. The native RCs were depleted up to 95% of both Q_A and Q_B by incubating the RCs in the presence of 4.5% LDAO, 10 mM *o*-phenanthroline, and 1 mM EDTA, according to the methods of Okamura et al. (1975) and Liu et al. (1991). Ten milliliters of 10 μM native RCs in TL buffer was added to 15 mL of Q-depletion column material, and the mixture was stirred gently for 10 min to allow the RCs to bind to the column material. It was put onto a column covered with a thin layer of DEAE-Sephacel and washed with 500 mL of Q-depletion solution at 26–28 °C. Then the temperature was lowered to 4 °C and the column was washed with 200 mL of TL buffer to remove the remaining *o*-phenanthroline. The Q-depleted RCs were eluted with 0.5 M NaCl in 10 mM Tris, 0.03% LDAO, and 1 mM EDTA and concentrated by ultrafiltration.

Reconstitution with Different Quinones. The depleted RCs were reconstituted at the Q_A- site with various quinones. The following quinones were used: anthraquinone (Fluka), 1-chloroanthraquinone (Aldrich), duroquinone (2,3,5,6-tetramethyl-1,4-benzoquinone, Sigma), 1,4-naphthoquinone (Sigma), menadione (2-methyl-1,4-naphthoquinone, Sigma), and ubiquinone-50 (2,3-dimethoxy-5-methyl-6-decaisoprenyl-1,4-benzoquinone, Sigma). The quinones were used for reconstitution without further purification. (The purity was checked by NMR spectroscopy.) MD was dissolved in distilled water and DQ and 1,4-NQ in absolute ethanol. AQ and 1-Cl-AQ were dispersed in dimethyl sulfoxide (DMSO) and UQ_{10} in 30% Triton X-100 (octylphenol poly(ethylene glycol) ether, Serva) detergent by sonication. The quinones were added to the RCs in ratios of Q/RC = 10 for UQ_{10} and Q/RC = 20 for the other quinones and incubated at 4 °C for 12 h. The

RCs were separated from the unbound quinones by DEAE-Sephacel chromatography. Before the measurement, the LDAO was changed to Triton X-100, and the buffer concentration was lowered by dialysis.

Q_A Content. The Q_A content of the preparations after depletion and subsequent reconstitution was assayed by flash-induced absorption change at 430 nm [$\Delta\epsilon(P^+Q_A^-/PQ_A) = 28$ mM^{-1} cm^{-1}; Maróti et al., 1985] or by cytochrome turnover at 550 nm [$\Delta\epsilon$(red/ox) = 21.1 mM^{-1} cm^{-1}; Van Gelder & Slater, 1962] measured on a kinetic spectrophotometer apparatus of local design. The decomposition of the $P^+Q_A^- \rightarrow PQ_A$ charge recombination kinetics into exponentials was based on the Marquardt nonlinear least-square method.

Proton Uptake Measurements. The light-induced proton uptake was determined by two different methods: optically with pH indicator dyes (bromocresol purple, Reanal, pH 5.5–7.5, λ = 579 nm; o-cresol red, Reanal, pH 7.0–9.0, λ = 562 nm; o-cresolphthalein, Reanal, pH 8.7–10.1, λ = 568 nm; tymolphthalein, Reanal, pH 9.5–10.4, λ = 569 nm) and electrically with a pH electrode (glass/Ag/AgCl combination semi-microelectrode, Corning No. 476540). The concentration of Tris buffer in the RC stock (10 mM) was decreased by overnight dialysis to a final concentration of 20 μM. Net proton binding was obtained by subtraction of the dye or pH electrode response in the unbuffered sample from that measured in the buffered (10 mM) solution. The following buffers were used at the indicated pH ranges: Bis-Tris (Sigma), pH 5.8–7.2; Mes (Sigma), pH 5.5–6.7; Hepes (Calbiochem-Behring), pH 7.0–8.0; Tris (Reanal), pH 7.8–8.8; Bis-Tris propane (Sigma), pH 6.5-9.5; Caps (Sigma), pH 9.7–11.1. The net responses were calibrated for quantities of H^+ ions by external acid (HCl) mixing. Absorption of carbon dioxide was prevented by flowing nitrogen gas over the sample. All measurements were carried out at room temperature except the thermal activation experiments in the physiological temperature range (4–35 °C).

RESULTS

Removal of Native Ubiquinone and Reconstitution of RCs with Various Quinones. The ubiquinone content of the RCs after preparation and purification was checked by functional assays of endogenous electron acceptor activity and was found to be around 1.6 UQ/RC, i.e., 60% of the RCs exhibited Q_B activity in the absence of added quinone. The quinone from the Q_B binding site could easily be extracted, but the removal of the ubiquinone from the Q_A binding site required more rigorous conditions (see Experimental Procedures). After depletion, the quinone content of the RC dropped to 0.05 UQ/RC.

In order to check for irreversible perturbations of structure and function due to the extraction and reconstruction procedures, we examined the behavior of the $P^+Q_B^- \rightarrow PQ_B$ back reaction, which is sensitive to small changes in the $Q_A^-Q_B \leftrightarrow Q_AQ_B^-$ equilibrium (Wraight & Stein, 1980; Kleinfeld et al., 1984b). The good agreement observed between the kinetics of the native and reconstituted RCs indicated that UQ_{10} could be incorporated efficiently into both quinone binding sites with essentially native behavior.

Electron Transfer Reactions. (A) pH Dependence of the Rate of Charge Recombination. The $P^+Q_A^- \rightarrow PQ_A$ back reaction can occur either directly (probably by a tunnelling mechanism) or indirectly by thermal activation to the relaxed state of P^+I^- (Arata & Parson, 1981; Gunner et al., 1982; Figure 1). The redox midpoint potential of the primary quinone acceptor determines which route will dominate. If we

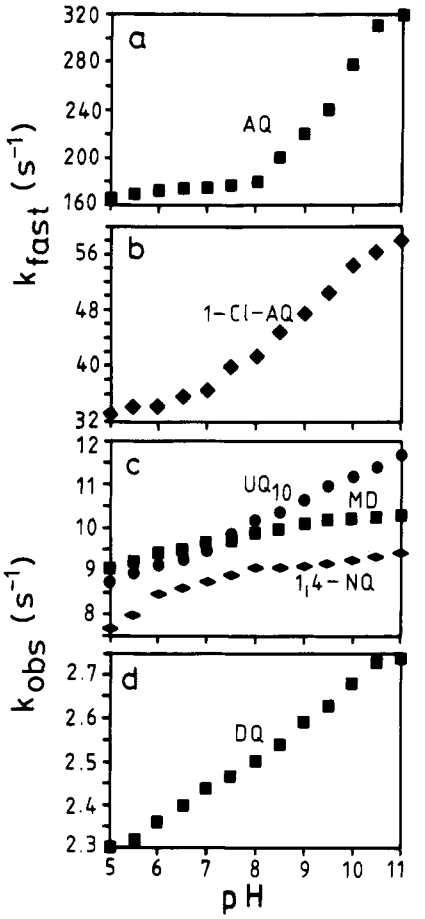

FIGURE 2: pH dependence of the rate of charge recombination $P^+Q_A^- \rightarrow PQ_A$ in reaction centers from *Rb. sphaeroides* of native Q_A (UQ_{10}) and quinone depleted and reconstituted with different quinones: DQ, 1,4-NQ, MD, AQ, and 1-Cl-AQ. The kinetic traces of absorption changes at 430 nm after a single saturating flash were decomposed into one (panels c and d) or two (slow and fast, panels a and b) components. Conditions: 1 μM RC, 10 mM buffer (Mes, Tris, or Caps, depending on pH), 100 mM NaCl, 0.03% Triton X-100, and +1 mM *o*-phenanthroline (native RC).

take 8×10^7 and 10 s^{-1} for the rates of $P^+I^- \rightarrow PI$ (Parson & Ke, 1982) and $P^+Q_A^- \rightarrow PQ_A$ direct back reactions (Figure 2 and Table 1), respectively, the two routes will be equally preferred if the free energy gap between P^+I^- and $P^+Q_A^-$ is 400 meV [see also Feher et al. (1988)]. From activation free energy measurements in AQ-substituted RC ($\Delta G° = 335$ meV at pH 8; see following sections) and the midpoint potential of the AQ in situ (E_m = –210 mV; Woodbury et al., 1986), a value of –545 meV can be calculated for the free energy level of the relaxed state of P^+I^-, which is in acceptable agreement with the –500 meV given by Sebban (1988a). This means that the back reaction in RCs with low-potential quinones ($E_m < -145$ mV) prefers the thermally activated route. On the other hand, the direct charge recombination dominates in RCs reconstituted with high-potential quinones ($E_m > -145$ mV). This corresponds to a free energy drop of $\Delta G°* = 765$ meV from the excited dimer P* (E_m= –910 mV), which is in good agreement with previous results ($\Delta G°* = 800$ meV; Woodbury et al., 1986).

The charge recombination after a single saturating flash excitation in RCs with substituted quinones at the Q_A site essentially followed this expectation. The kinetics were monoexponential, temperature-independent, and very weakly pH-dependent for the native (UQ_{10}) and DQ-, 1,4-NQ-, and MD-substituted RCs (Figure 2 and Table 1). The observed biexponentiality was about 5% and was attributed to the

Table 1: Electro- and Photochemical Properties of Quinones Used for the Reconstitution of Q_A-Depleted RCs of *Rb. sphaeroides*

quinones	E_m in DMF (mV)[a]	E_m in situ (meV)[a]	$\Delta G°$ (meV)[b]	$k_{P^+Q^-}$ (s^{-1})[c] pH 6	$k_{P^+Q^-}$ (s^{-1})[c] pH 11	A_{slow}/A_{fast} + A_{slow}[d]	T_{PQ^-} (s)[e] pH 6	T_{PQ^-} (s)[e] pH 9	pK_a[f]	$\Delta G_H°$ (meV)[g] pH 5
UQ_{10}	−600	−50	910	8.5	11.7	1	60	45	5.9*	−101
DQ	−750	−20	940	2.3	2.73	0.95	10.4	4.5	5.1	−86
1,4-NQ	−590	−60	900	7.7	9.4	0.95	2.5	1.9	4.1	−64
MD	−640	*80	880	9.1	10.3	0.95	10.0	9.3	4.5	−49
1-Cl-AQ	−750	−170	790	33	58*	0.5–0.35*	4.0	3.0	ND	−79
AQ	−830	−210	700	165	320*	0.4–0.2*	ND	ND	5.3	−82

[a] Redox midpoint potentials of quinones in dimethylformamide (DMF) and in situ (Woodbury et al., 1986). [b] Free energy difference between P^*Q_A and $P^+Q_A^-$. [c] Rate constants of charge recombination $P^+Q_A^- \rightarrow PQ_A$ calculated from exponential analysis (see Experimental Procedures) (*, rate constants of the fast components). [d] Fraction of the slow component (*, depending on pH). [e] Lifetime of PQ_A^- state (in the presence of 200 μM ferrocene). [f] pK_a values of the semiquinones in aqueous solution (except * in 7 M isopropyl alcohol and 1 M acetone (Swallow, 1982). ND, data not available. [g] pH-dependent stabilization energy determined by integrated proton uptake (see Figure 6).

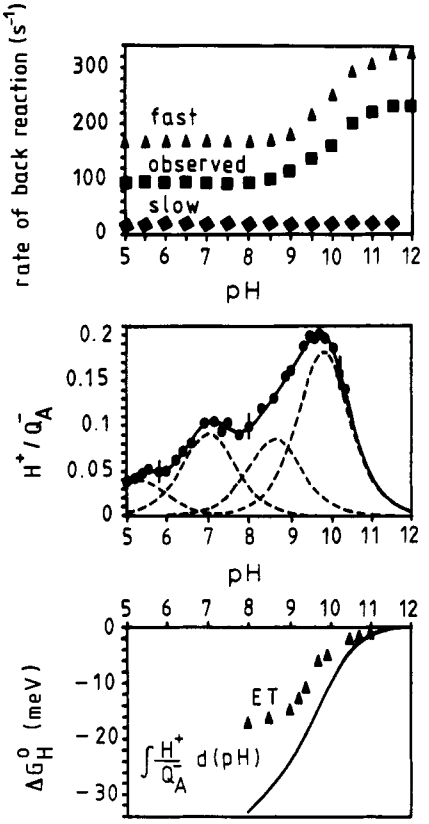

FIGURE 3: Connection between the rate of electron transfer ($P^+Q_A^- \rightarrow PQ_A$ recombination, top), proton binding stoichiometry, H^+/Q_A^-, associated with the $PQ_A \rightarrow P^+Q_A^-$ transition (middle), and stabilization energy, $\Delta G_H°$, due to the protonation (bottom) of AQ-reconstituted RC in the alkaline pH range. The pH dependence of the stabilization energy was calculated (A) from integration of the proton binding stoichiometry as a function of pH [(−59 meV)$\int(H^+/Q_A^-)$ d(pH) (continuous line)] and (B) from thermal activation of the fast component of the electron transfer [(−25 meV)ln k_H/k_o, where k_H and k_o are the rates of recombination at arbitrary pH and very high pH (>11.5), respectively (▲)].

residual level of unextracted RCs. The case with substitution of low-potential quinones (AQ and 1-Cl-AQ) was more complex. The observed back-reaction kinetics was significantly biphasic and pH-dependent (Figures 2 and 3, top). The fast component reflected the indirect recombination path, as its rate was pH and temperature-dependent in contrast to the slow phase. The rate of the fast phase was clearly under the control of a protonatable group with a pK of about 9.8, as was observed earlier by Kleinfeld et al. (1985) and Sebban (1988b).

The activation parameters of the $P^+Q_A^- \rightarrow PQ_A$ charge recombination were determined from Arrhenius plots and are summarized in Table 2. For AQ-substituted RCs, the activation enthalpies were 370 (pH 7.0) and 325 meV (pH 10.0) and the free energy changes of activation were 340 (pH 7.0) and 320 meV (pH 10.0). These data are in good agreement with those obtained by Woodbury et al. (1986) from delayed fluorescence measurements at pH 8.0. The entropic contribution to the free energy changes is overwhelmed by the much larger enthalpy change. The entropic term shows a slight variation upon pH change: it is smaller at high pH than at neutral pH. The observed tendency can be rationalized in terms of proton binding stoichiometries, which show similar changes at these pH values. Arata and Parson (1981) suggested that dielectric relaxation, including protonation events and the accompanying changes in charge and solvent mobility, was associated with entropic effects.

Table 2: Activation Parameters of the Charge Recombination and H^+ Ion Binding Stoichiometry (H^+/Q_A^-) of AQ-Reconstituted RC of *Rb. sphaeroides* at Neutral and Alkaline pH Values

pH	$\Delta H°$ (meV)[a]	$T\Delta S°$ (meV)[a,b]	$\Delta G°$ (meV)[a,b]	H^+/Q_A^-[c]
7.0	370 ± 30	32 ± 10	340 ± 30	0.30
10.0	325 ± 30	6 ± 10	320 ± 30	0.18

[a] $\Delta H°$, $\Delta S°$, and $\Delta G°$ are the changes of enthalpy, entropy, and free energy of activation, respectively. The errors for the Arrhenius plots in the ambient temperature range (273–310 K) were given by least-squares analysis. [b] T = 293 K. [c] Proton uptake in the presence of 200 μM ferrocene.

The amplitude of the slow component in the biexponential analysis of the AQ-reconstituted RCs was significantly greater than 5% of RCs still containing ubiquinone. It could not originate from AQ on the Q_B- site (AQ was added in excess of the RC) as the slow phase was insensitive to terbutryn, a potent inhibitor of the interquinone electron transfer. Furthermore, there is no second turnover of the RCs under repetitive saturating flash excitation (Figure 4). Similar kinetic complexity was observed by Woodbury et al. (1986), but was not reported by Kleinfeld et al. (1985) and Sebban (1988b). In RCs reconstituted with 1-Cl-AQ, the fraction of the slow phase was even larger and reached 50% at pH 8. It can be attributed to the non-negligible contribution of the direct pathway in recombination because the energy levels of these quinones are close to the value of equal participation of the two routes (see above). One can speculate further about the heterogeneity (position, orientation, etc.) of quinones in the reconstituted RCs, which might cause a distribution of rates in the direct recombination process (Woodbury et al., 1986; Allen et al., 1988; Maróti, 1993).

(B) Lifetime of the Q_A^- State. In RCs lacking functional Q_B, the lifetime of the semiquinone is determined by charge recombination and falls in the 1–500-ms time interval, depending on the type of quinone. To avoid kinetic limitations in semiquinone-induced protonation or experimental techniques (pH electrode), extended semiquinone lifetimes are useful. This can be achieved by fast external donors (ferrocene

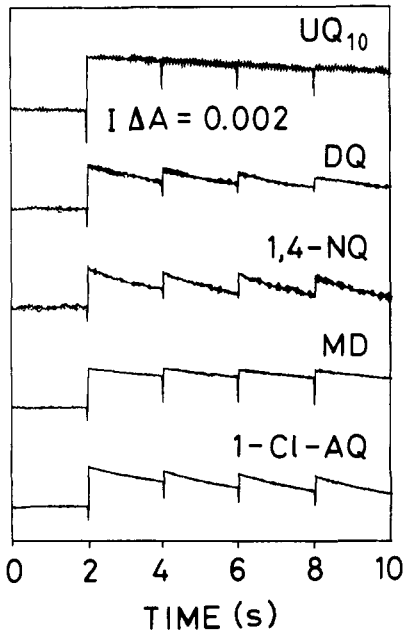

FIGURE 4: Tracking of semiquinones at 450 nm in native (Q_A = UQ_{10}) and depleted and reconstituted (QA = DQ, 1,4-NQ, MD, and 1-Cl-AQ) RCs of *Rb. sphaeroides* exposed to a series of saturating flashes (0.5 Hz). Conditions: 1 μM RC, 10 mM Mes, pH 6.0, 100 mM NaCl, 0.03% Triton X-100, and 200 μM ferrocene.

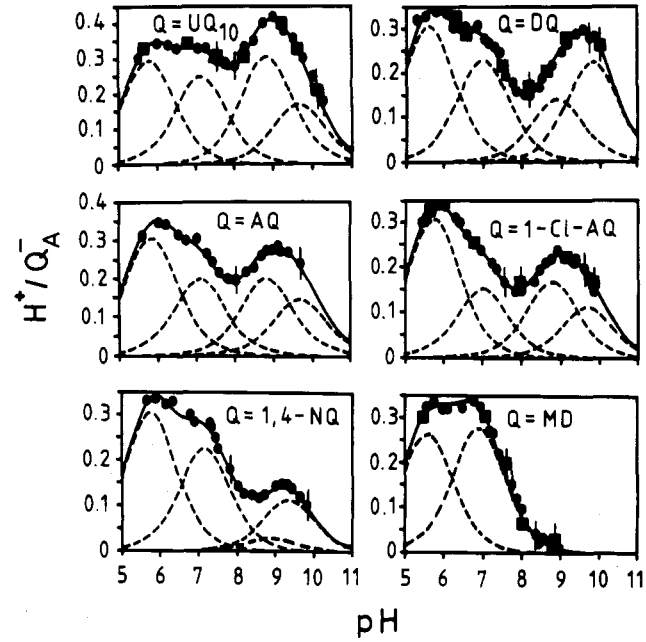

FIGURE 5: pH dependence of the proton binding stoichiometry associated with the $Q_A \rightarrow Q_A^-$ flash-induced transition in native (Q_A = UQ_{10}) and (after depletion) reconstituted (QA = DQ, 1,4-NQ, MD, AQ, and 1-Cl-AQ) RCs of *Rb. sphaeroides* using spectrophotometric (●) and pH electrode (■) assays. The proton binding of AQ-substituted RCs was determined from proton uptake due to the $PQ_A \rightarrow P^+Q_A^-$ transition (Figure 3, middle) and corrected for $P \rightarrow P^+$ proton release (Maróti & Wraight, 1988; McPherson et al., 1988). The observed proton binding is approximated by the sum (—) of Henderson–Hasselbalch-type curves (- - -) representing the contribution of protonatable residues (see details in Table 3). Error bars show the estimated statistical errors. Conditions: 2 μM RC, 100 μM/10 mM buffer (see Experimental Procedures), 0.03% Triton X-100, 50 mM NaCl, 200 μM ferrocene, and 40 μM pH indicator dye (in the case of the spectrophotometric method).

in large (>100 μM) concentration) to re-reduce the oxidized dimer before the back reaction takes place. In this case, the semiquinone has a much longer lifetime because its rate of reoxidation depends on the accessibility of external oxidants (Figure 4). The lifetimes of the different semiquinones are pH-dependent and range from a few seconds (1,4-NQ, 1-Cl-AQ, MD, and DQ) to minutes (UQ_{10}) (Table 1).

Stoichiometry of Proton Binding. Two methods (spectrophotometric and pH electrode methods) were used to determine the stoichiometry of flash-induced proton uptake in RCs substituted with different quinones at the Q_A^- site in the pH range 5–11. Due to their different sensitivities and kinetic responses (Maróti, 1993), the two techniques were complementary to each other and showed satisfactory agreement under similar (overlapping) conditions.

The observed proton uptake was normalized to the concentration of the charge-separated state $P^+Q_A^-$ determined from optical absorbance changes at 430 nm (Maróti et al., 1985). The proton uptake of RCs reconstituted by UQ_{10} agreed well with that of native RC measured earlier (Maróti & Wraight, 1988; McPherson et al., 1988). The proton binding was a small fraction of a proton over the whole pH range, indicating weak interaction of the different semiquinones with the protonatable amino acids of the protein (Figures 3 (middle) and 5). The stoichiometries were decomposed into the sum of contributions of individual protonatable residues (Table 3). Except for MD, a minimum number of four groups was required to obtain acceptable fits over the whole pH range, in agreement with previous results (Maróti & Wraight, 1988; McPherson et al., 1988; Maróti, 1993).

(A) H^+ Ion Binding to the $P^+Q_A^-$ State. Due to the short lifetimes of the semiquinones, only pH indicator dyes could be used. The pH dependence of the stoichiometry of proton binding is significantly modified by the proton release from oxidized dimer (Figure 3, middle). As a result, the observed proton binding decreases at the acidic and neutral pH ranges, but the effect on the high-pH behavior of the protonation is negligible. This is in accordance with earlier measurements on native RCs (Maróti & Wraight, 1987, 1988; McPherson et al., 1988).

Table 3: List of pK Values of Protonatable Amino Acids (Groups 1–4) in the Oxidized (pK_Q) of Reduced (pK_{Q^-}) States of Different Quinones in the Q_A Binding Pocket

	group 1[a]		group 2[a]		group 3[a]		group 4[a]	
quinones	pK_Q	pK_{Q^-}	pK_Q	pK_{Q^-}	pK_Q	pK_{Q^-}	pK_Q	pK_{Q^-}
UQ-50	5.52	6.05	6.90	7.35	8.55	9.10	9.50	9.80
DQ	5.30	5.85	6.77	7.18	8.75	9.00	9.60	10.00
1,4-NQ	5.45	6.00	6.95	7.35	8.80	8.85	9.20	9.40
MD	5.30	5.77	6.60	7.10				
1-Cl-AQ	5.45	6.00	6.70	7.12	8.60	8.90	9.55	9.75
AQ	5.55	6.02	6.85	7.35	8.61	8.91	9.55	9.78
P(AQ)/P$^+$(AQ)$^-$	5.30	5.37	6.95	7.11	8.55	8.7	9.65	9.97

[a] The pK values were obtained by analysis of proton binding stoichiometries (Figure 5) in terms of single titration curves.

(B) H^+ Ion Binding to the PQ_A^- State. The PQ_A^- state is especially suited to studies of semiquinone-linked proton uptake, as the pH electrode technique can also be used and the contribution of P^+-related proton unbinding is avoided. There is no major change in the proton uptake for the various quinones in the acidic range (5.5 < pH < 7, Figure 5). A local minimum can be found around pH 8 and a maximum between pH 9 and 10. However, significant changes can be observed in the alkaline pH range. In RCs with quinones having one ring, UQ_{10} and DQ, the maxima are 0.4 and 0.3 H^+/Q_A^-, respectively. A somewhat smaller proton uptake (0.25 H^+/Q_A^-) was measured in RCs where the quinones contained three rings (AQ and 1-Cl-AQ). The smallest proton uptake was observed in RCs reconstituted with quinones

Table 4: Protonatable Amino Acids Closer Than 18 Å to Q_A in RC of *Rb. sphaeroides*

distance from Q_A[a]	Glu[b]	Asp	Cys	Tyr	Arg
12–13	H38				M253
13–14	M246, M263		L108	H40	
14–15				L9	
15–16	H34				M241, M247
16–17	L212			H30	M267
17–18	M232	H231			M228, H37

[a] Distances between the geometric center of the ring of UQ_0 (Q_A) and the protonatable atoms were calculated from the coordinates of the crystal structure (Armoux et al., 1989). [b] Glu M234 (10.0 Å) and Glu L104 (11.7 Å) were omitted because of a bidental ligand to Fe^{2+} and an H-bond to bacteriopheophytin, respectively.

containing two rings: 0.15 H^+/Q_A^- for 1,4-NQ and no proton for MD above pH 9. In the latter case, the proton binding stoichiometry can be described by only two protonatable groups over the whole pH range.

DISCUSSION

The protonation site in the vicinity of Q_A was probed by charge recombination and direct proton binding, with the native ubiquinone replaced by a variety of benzo-, naphtho-, and anthraquinones. The results are a rich source of information on the energetics of the quinones, as the rate of the thermally activated back reaction (indirect route) and the proton binding stoichiometry are sensitive to small perturbations in the free energy of Q_A^- caused by electrostatic interactions with protonatable residues in its vicinity.

Stabilization of Q_A^- by Proton Binding. Charges on amino acids of the protein can modify the energy of Q_A^- in various ways. Easily polarizable amino acids and positively charged residues lower the energy of the semiquinone. However, there are no such groups within a 12-Å distance from Q_A (Table 4). The presence of a negative charge on the carboxylic groups would raise the energy of Q_A^-, but these acidic residues may become protonated, in which case they lower the energy of Q_A^-. The number of Asp and Glu residues is especially high in the H subunit, as high as those of the L and M subunits together (29). On the basis of the structural data, one can expect that the stabilization of the semiquinone as a function of pH is controlled by the protonation of the amino acid residues. In that case, the lowering of the free energy can be obtained directly from the integrated proton uptake (Feher et al., 1988; McPherson et al., 1988, 1990).

(A) Low-Potential Quinones (AQ). The charge-separated state of AQ-reconstituted RCs has the advantage that due to the thermal activation of the fast phase of the recombination, the energy of stabilization can be determined by two independent methods (Figure 3). Similar studies were carried out for Q_B^- stabilization in native RCs (McPherson et al., 1988). The pH dependencies of the free energy changes calculated by the two methods are in reasonable agreement above pH 9. The deviation becomes more significant below pH 9, where greater stabilization energy can be deduced from proton binding than from the electron transfer data. One can argue that, upon lowering of the pH, the stabilization of the semiquinone will be so large (82 meV at pH 5) that a clear distinction between the indirect and other (direct) routes based on decomposition of the charge recombination kinetics becomes more difficult.

(B) High-Potential Quinones. The pH dependencies of the stabilization energy for different quinones are shown in Figure 6. They were calculated from the integrated proton binding stoichiometry. The free energy change is largest for

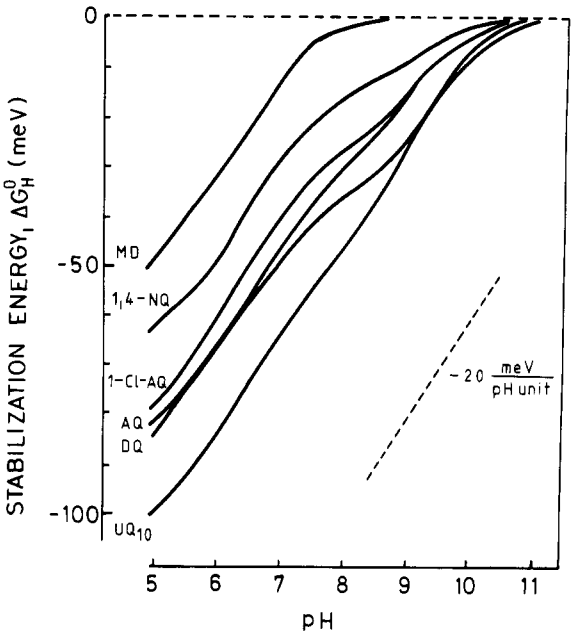

FIGURE 6: pH dependence of the stabilization energy of RCs from *Rb. sphaeroides* reconstituted with different quinones in the Q_A binding site, calculated by integration of the proton binding stoichiometry (Figure 5) as a function of pH (see the legend for Figure 3). The average slope of –20 mV/pH unit is indicated by the dashed line.

Scheme 1

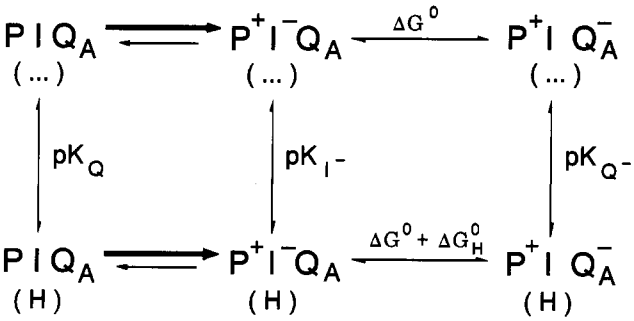

the native ubiquinone (100 meV at pH 5) and smallest for MD (49 meV at pH 5). The overall slope is about –20 meV/pH unit for all quinones, which corresponds to 0.3 H^+/e^-. This means that the various quinones at the Q_A site have about the same interactions with all of the protonatable residues except for one in the high-pH region (see also the list of the pK's of protonatable groups determined from a phenomenological model; Table 3). The assignment of this group will be discussed later.

Consequences of Proton Uptake on P^+I^- Stabilization. We can utilize the detailed energetic description of the AQ-substituted RCs for the estimation of the interaction energy between the high-pH residue and the reduced bacteriopheophytin. For this single protonation site, the correlation among the light-driven reaction (heavy arrow), electron transfer (horizontal direction), and protonation (vertical direction) can be represented as shown in Scheme 1. $\Delta G°$ and $\Delta G° + \Delta G_H°$ are the free energy gaps for the electron transfer at high- and low-pH limits when the closely spaced protonatable group is fully ionized and fully protonated, respectively. pK_Q, pK_{I^-}, and pK_{Q^-} are the pK values for the group when Q_A and I are in their oxidized states, I is in its reduced state, and Q_A is in its semireduced state, respectively. As the lifetime of $P^+IQ_A^-$ (see Table 1) is much larger than the time for protein relaxation (about 200 μs at pH 7; Brzezinski et al., 1992;

Tiede & Hanson 1992) or protonation (Maróti & Wraight, 1989; Maróti, 1991b), thermal equilibrium is achieved for both protonation and electron transfer before the flash (dark state) and after the flash (charge-separated state). According to the law of energy conservation, the sum of free energy changes among different species in the charge-separated state should be zero. From this relationship, we can calculate pK_{I^-} from the other energetic parameters: $pK_{I^-} = pK_{Q^-} - \Delta G_H^\circ/(59\ \text{meV})$. Taking $\Delta G_H^\circ = 18$ meV (Figure 3, bottom) and $pK_{Q^-} = 9.9$ (Table 3), we obtain $pK_{I^-} = 9.6$, which corresponds to the dark pK value of the residue: $pK_{I^-} = pK_Q$ (see Table 3). Although there is no experimental way to prolong the lifetime of the P^+I^- state as long as protonation could take place, it can be concluded from energetic considerations that no protonation would occur because the interaction between P^+I^- and the high-pH protonatable group is negligible. Similar conclusions can be drawn from earlier studies on the pH dependence of $P^+Q_A^-$ recombination in RCs of *Rhodopseudomonas viridis*. Shopes and Wraight (1987) derived pK values of approximately 9.4 (pK_{I^-}) and approximately 9.7 (pK_{Q^-}) indicating that the high-pH group had a stronger interaction with Q_A^- than with I^-. Sebban and Wraight (1989) assumed two protonatable groups: one with pK_Q about 6, for which protonation resulted in the relative stabilization of P^+I^-, and one with pK_Q about 9, which relatively stabilized $P^+Q_A^-$ in the protonated state.

Assignment of the High-pH Protonatable Group. The protonation sites for Q_A can be located either at longer distance, at the Q_B binding site, or in closer vicinity of the Q_A binding pocket. It has been suggested previously that the same residue may be involved in redox-linked protonation for both Q_A/Q_A^- and Q_B/Q_B^-, with somewhat different pK values of 9.8 and 11.3, respectively (Kleinfeld et al., 1984b, 1985; Maróti & Wraight, 1987). Site-directed mutation studies have strongly implicated the involvement of Glu L212, with an unusually high pK (=9.6), in the proton binding behavior of Q_B at high pH (Paddock et al., 1989; Takahashi & Wraight, 1992). It has been shown that the protonation state of Glu L212 probably influences the conformational change upon formation of Q_A^- (Brzezinski et al., 1992). The arguments indicate a weak (long-range) electrostatic interaction between the two quinone binding pockets. Although the distance between Glu L212 and the center of the ring of Q_A is fairly large (16.5 Å), the contribution of Glu L212 in the high-pH proton binding attributed to Q_A reduction is highly probable.

On the basis of the structure of atomic resolution (Arnoux et al., 1989), we collected the protonatable amino acids that are closer to the center of the ring of Q_A than 18 Å (Table 4). Among the residues with pK_a values not in the far alkaline pH range and closest to Q_A, Cys L108 (14.0 Å) and Tyr H40 (13.5 Å) can be involved in the discussion. The expected pK_a values of cysteine in proteins (8.2–8.6) are significantly lower than 9.6, but typical pK_a values of tyrosine in proteins range from 9.6 to 10.0 (Cantor & Schimmel, 1980). Tyr H40 seems to be an appropriate candidate for controlling the high-pH behavior of semiquinone stabilization. It is at the surface of the protein and exposed to the water phase (Figure 7).

If we assume a simple Coulombic electrostatic interaction between Q_A^- and the protonatable oxygen atom of Tyr H40 at a distance of 13.5 Å, the effective dielectric constant should be $\epsilon_{eff} = 52$ to explain the observed $pK_{Q^-} - pK_Q = 0.3$ shift in pK values (Table 3). A similar calculation for Glu L212 gives $\epsilon_{eff} = 43$. These values are in reasonable agreement with the general electrostatic behavior of proteins. The protein cannot be treated as a low-dielectric medium, and the effective

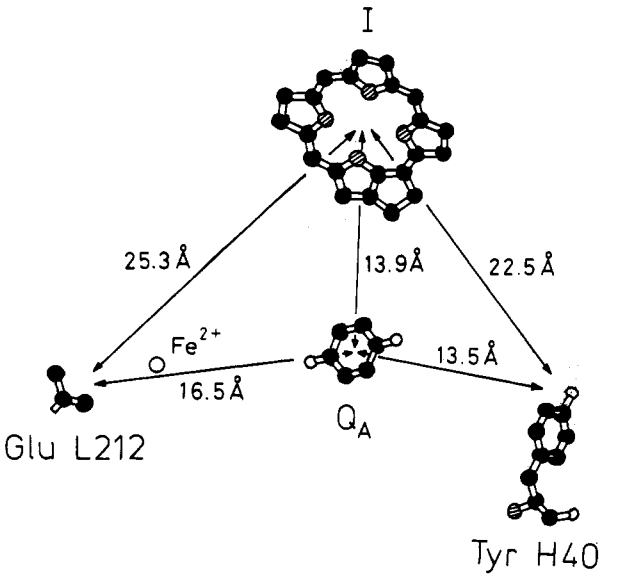

FIGURE 7: Relative positions of the primary quinone (Q_A), bacteriopheophytin (I), non-heme iron (Fe^{2+}), Tyr H40, and carboxyl group of Glu L212 in RC of *Rb. sphaeroides*. The hydrocarbon side chains of Q_A and I are omitted. The numbers above the arrowed lines show center to center (Q_A and I) and center to protonatable atom (Tyr H40 and Glu L212) distances. (X-ray crystallographic coordinates were kindly provided by B. Arnoux and F. Reiss-Husson.)

dielectric constant is large at equilibrium. The empirical and distance-dependent expression of the dielectric constant introduced by Warshel and Russel (1984) offers $\epsilon_{eff} = 44 \pm 22$ at 13.5-Å (Tyr H40) and $\epsilon_{eff} = 48 \pm 24$ at 16.5-Å (Glu L212) distances.

Semiquinone and Its Environment in RC. The conformational modifications necessary for exchanging the quinone in the Q_A site are largely reversible, and the photochemical activity could be restored completely. We cannot be sure, however, to what extent the environment of the exchanged quinones remains unperturbed. Redox, acid/base, and geometrical properties of the semiquinone may modify the environment, which is reflected in changes in the stabilization energies. A useful indication can be the differences in redox midpoint potentials measured in situ and in organic solvent (DMF) for the different quinones (Table 1). Although the shifts are considerable, they do not show significant specificity (730 meV for DQ and 530–580 meV for the others).

Some of the added quinones are bulkier than ubiquinone and are expected to fit into the Q_A binding pocket in different ways. The size of the ring system can cause minor modifications not only in the environment but also in the distance to the protonatable groups via different delocalization of the electron in the semiquinone. The two types of contributions are difficult to separate, and this could be the reason why the correlation between the observed changes in the proton binding stoichiometries (Figure 5) and the geometrical sizes of the ring systems is not very strong.

To rationalize the extent of delocalization of the electron in the ring systems of the quinones, the pK values of their semiquinone forms can be compared (Swallow, 1982). The pK values of semiquinones are consistent with the electron-donating properties of the side groups and, thus, with the electron density at the center of the ring. The lower the pK, the smaller the electron density on the ring. Among the quinones used in this study (Table 1), 1,4-NQ has the lowest pK (4.1) because it contains a less electron-donating group. The pK of MD (4.5) is somewhat larger due to the methyl group, which donates electrons into the ring. The other

quinones all have larger pK values in their semiquinone forms. The small differences in electron delocalization over the ring systems of different types of semiquinones can result in changes in interaction with closely spaced protonatable amino acids, but may not have any effect on interactions with distant groups. This is in reasonable agreement with the high-pH behavior of the observed proton binding (Figure 5). Semiquinones of 1,4-NQ and MD in the Q_A binding site show significantly weaker interactions with the (closely spaced) high-pH residue (pK = 9.6) than all other semiquinones (Table 3). The proton binding stoichiometry over the acidic and neutral pH ranges, however, is determined by interactions with distant groups that are not sensitive to the delocalization of electrons in the ring system. Consequently, no significant changes can be measured due to the differences in the ring sizes of the quinones.

The explanation of the different stabilization energies of the quinones in the Q_A site may lie partly in the physicochemical properties of the quinones and partly in subtle structure alterations. High-resolution atomic structures of reconstituted RCs would certainly help in the identification of changes in the environment, but presently they are not readily obtainable.

ACKNOWLEDGMENT

We thank Drs. P. Sebban and C. A. Wraight for helpful discussions, B. Arnoux and F. Reiss-Husson for the reaction center coordinates, and G. Horváth for his valuable help in RC preparation.

REFERENCES

Allen, J. P., Feher, G., Yeates, T. O., Komiya, H., & Rees, D. C. (1987) *Proc. Natl. Acad. Sci. U.S.A. 84*, 5730–5734.
Allen, J. P., Feher, G., Yeates, T. O., Komiya, H., & Rees, D. C. (1988) *Proc. Natl. Acad. Sci. U.S.A. 85*, 8487–8491.
Arata, H., & Parson, W. W. (1981) *Biochim. Biophys. Acta 638*, 201–209.
Arnoux, B., Ducruix, A., Reiss-Husson, F., Lutz, M., Norris, J., Schiffer, M., & Chang, C.-H. (1989) *FEBS Lett. 258*, 47–50.
Brzezinski, P., Okamura, M. Y., & Feher, G. (1992) in *The Photosynthetic Bacterial Reaction Center II* (Breton, J., & Vermeglio, A., Eds.) pp 321–330, Plenum Press, New York.
Cantor, Ch. R., & Schimmel, P. R. (1980) in *Biophysical Chemistry*, Part I, pp 41–53, W. H. Freeman and Company, San Francisco.
Chang, C.-H., Tiede, D., Tang, J., Smith, U., Norris, J., & Schiffer, M. (1986) *FEBS Lett. 205*, 82–86.
Clayton, R. K., & Straley, S. C. (1972) *Biophys. J. 12*, 1221–1234.
Feher, G., Arno, T. R., & Okamura, M. Y. (1988) in *The Photosynthetic Bacterial Reaction Center* (Breton, J., & Vermeglio, A., Eds.) pp 271–287, Plenum Press, New York.
Gunner, M. R., & Honig, B. (1992) in *Photosynthetic Bacterial Reaction Center II* (Breton, J., & Vermeglio, A., Eds.) pp 403–410, Plenum Press, New York.
Gunner, M. R., Tiede, D. M., Prince, R. C., & Dutton, P. L. (1982) in *Function of Quinones in Energy Conserving Systems* (Trumpower, B. L., Ed.) pp 265–269, Academic Press, Inc., New York.
Gunner, M. R., Robertson, D. E., & Dutton, P. L. (1986) *J. Phys. Chem. 90*, 3183–3195.
Hanson, D. K., Tiede, D. M., Nance, S. L., Chang, C.-H., & Schiffer, M. (1993) *Proc. Natl. Acad. Sci. U.S.A. 90*, 8929–8933.
Kálmán, L., Turzó, K., & Maróti, P. (1993) *Photosynthetica 28* (2), 185–194.
Kleinfeld, D., Okamura, M. Y., & Feher, G. (1984a) *Biochemistry 23*, 5780–5786.
Kleinfeld, D., Okamura, M. Y., & Feher, G. (1984b) *Biochim. Biophys. Acta 766*, 126–140.
Kleinfeld, D., Okamura, M. Y., & Feher, G. (1985) *Biophys. J. 48*, 849–852.
Liu B.-L., Yang L.-H., & Hoff, A. J. (1991) *Photosynth. Res. 28*, 51–58.
Maróti, P. (1991a) *J. Photochem. Photobiol. B: Biol. 8*, 263–277.
Maróti, P. (1991b) *Photosynthetica 25* (2), 173–180.
Maróti, P. (1993) *Photosynth. Res. 37*, 1–17.
Maróti, P., & Wraight, C. A. (1987) in *Progress in Photosynthesis Research* (Biggins, J., Ed.) Vol. II, pp 401–404, Martinus Nijhoff, Dordrecht, The Netherlands.
Maróti, P., & Wraight, C. A. (1988) *Biochim. Biophys. Acta 934*, 329–347.
Maróti, P., & Wraight, C. A. (1989) *Biophys. J. 55, 428a* (abstract).
Maróti, P., Kirmaier, Ch., Wraight, C. A., Holten, D., & Pearlstein, R. M. (1985) *Biochim. Biophys. Acta 810*, 132–139.
Maróti, P., Hanson, D. K., Baciou, L., Schiffer, M., & Sebban, P. (1994) *Proc. Natl. Acad. Sci. U.S.A.* (in press).
McPherson, P. H., Okamura, M. Y., & Feher, G. (1988) *Biochim. Biophys. Acta 934*, 348–368.
McPherson, P. H., Nagarajan, V., Parson, W. W, Okamura, M. Y., & Feher, G. (1990) *Biochim. Biophys. Acta 1019*, 91–94.
Okamura, M. Y., & Feher, G. (1992) *Annu. Rev. Biochem. 61*, 861–896.
Okamura, M. Y., Isaacson, R. A., & Feher, G. (1975) *Proc. Natl. Acad. Sci. U.S.A. 72*, 3491–3495.
Paddock, M. L., Rongey, S. H., Feher, G., & Okamura, M. Y. (1989) *Proc. Natl. Acad. Sci. U.S.A. 86*, 6602–6606.
Parson, W. W., & Ke, B. (1982) in *Photosynthesis* (Govindjee, Ed.) Vol I, pp 331–385, Academic Press, Inc., New York.
Sebban, P. (1988a) *FEBS Lett. 233* (2), 331–334.
Sebban, P. (1988b) *Biochim. Biophys. Acta 936*, 124–132.
Sebban, P., & Wraight, C. A. (1989) *Biochim. Biophys. Acta 974*, 54–65.
Shopes, R. J., & Wraight, C. A. (1987) *Biochim. Biophys. Acta 893*, 409–425.
Swallow, A. J. (1982) in *Function of Quinones in Energy Conserving Systems* (Trumpower, B. L., Ed.) pp 59–72, Academic Press, Inc., New York.
Takahashi, E., & Wraight, C. A. (1992) *Biochemistry 31*, 855–866.
Tiede, D. M., & Hanson, D. K. (1992) in *Photosynthetic Bacterial Reaction Center II* (Breton, J., & Vermeglio, A., Eds.) pp 341–350, Plenum Press, New York.
Van Gelder, B. F., & Slater, E. C. (1962) *Biochim. Biophys. Acta 58*, 593–595.
Warshel, A., & Russel, S. T. (1984) *Q. Rev. Biophys. 17*, 283–422.
Woodbury, N. W., Parson, W. W., Gunner, M. R., Prince, R. C., & Dutton P. L. (1986) *Biochim. Biophys. Acta 851*, 6–22.
Wraight, C. A., & Stein, R. R. (1980) *FEBS Lett. 113*, 73–77.